Rapid Early Holocene Deglaciation Of The Laurentide Ice Sheet

Anders E. Carlson[1]*, Allegra N. LeGrande[2], Delia W. Oppo[3], Rosemarie E. Came[4],

Gavin A. Schmidt[2], Faron S. Anslow[5], Joseph M. Licciardi[6], Elizabeth A. Obbink[1]

[1] *Department of Geology & Geophysics, University of Wisconsin, Madison, WI, 53706,*

USA

[2] *NASA Goddard Institute for Space Studies and Center for Climate System Research,*

Columbia University, New York, NY, 10025, USA

[3] *Department of Geology and Geophysics, Woods Hole Oceanographic Institution,*

Woods Hole, MA 02543, USA

[4] *Geology & Planetary Sciences, California Institute of Technology, Pasadena, CA,*

91125, USA

[5] *Earth and Ocean Sciences, University of British Columbia, Vancouver, BC, V6T 1Z4,*

Canada

[6] *Department of Earth Sciences, University of New Hampshire, Durham, NH, 03824,*

USA

*corresponding author: acarlson@geology.wisc.edu, 608-262-1921

The early Holocene deglaciation of the Laurentide Ice Sheet (LIS) is the most recent and best constrained disappearance of a large Northern Hemisphere ice sheet. Its demise is a natural experiment for assessing rates of ice sheet decay and attendant contributions to sea level rise. Here we demonstrate with terrestrial and marine records that the final LIS demise occurred in two stages of rapid melting from ~9.0-8.5 and 7.6-6.8 kyr BP with the LIS contributing ~1.3 and 0.7 cm yr^{-1} to sea level rise, respectively. Simulations using a fully coupled atmosphere-ocean general circulation model suggest that increased ablation from enhanced early Holocene

boreal summer insolation may have been the predominant cause of the LIS contributions to sea level rise. Although the boreal summer surface radiative forcing of early Holocene LIS retreat is twice that of projections for 2100 C.E. greenhouse gas radiative forcing, the associated summer surface air temperature increase is the same. The geologic evidence for rapid LIS retreat under a comparable forcing provides a prehistoric precedent for a possible large negative mass balance response of the Greenland Ice Sheet by the end of the coming century.

One of the greatest sources of uncertainty in projections of future sea level rise in response to global warming is the melt contribution from the Greenland Ice Sheet[1]. This uncertainty arises in part because the period of direct observations available to create empirical predictions and to test the current generation of ice sheet models is extremely short[1-5]. Examination of past ice sheet-climate interactions provides a record of ice sheet growth and decay longer than modern observations. In particular, the behavior of terrestrial ice sheets under climates warmer than present affords potential insight into the future behavior of the Greenland Ice Sheet. During the early Holocene, enhanced boreal summer insolation[6] (Fig. 1a) warmed Northern Hemisphere summers by several degrees, presumably driving retreat of the Laurentide Ice Sheet (LIS)[7-9]. However, portions of the northern and eastern North Atlantic were colder than present[10-12], possibly as a consequence of the suppression of Labrador Sea deep water production by LIS meltwater[13,14]. The gradual rise in sea level during the early Holocene[15-17] was punctuated by at least two increases in the rate of sea level rise, which were sourced from either the LIS or Antarctic Ice Sheet, indicating variations in the rate of ice sheet melting[14,18,19]. The early Holocene LIS thus represents the most recent disappearance of a mid- to high-latitude terrestrial ice sheet, and can provide constraints on how fast

terrestrial ice sheets can melt and raise sea level under a climate warmer than present.

Early Holocene Laurentide Ice Sheet Retreat

To determine the LIS retreat rate, we compiled minimum limiting radiocarbon dates of deglaciation for Quebec, Labrador, eastern Nunavut[20] and Hudson Bay[21], along with cosmogenic [10]Be ages from Labrador[22] and Quebec[14] (Fig. 1c, 2a & S1). All radiocarbon ages are calibrated, reservoir corrected if marine[20,21] (Table S1), and presented as straight averages of the oldest dates, which constrain deglaciation as occurring sometime before the deposition of the organic material or shell.

Four marine shell dates place the marine incursion following deglaciation of the northern bank of the St. Lawrence estuary at 11.8±0.3 kyr BP (Fig. S1). The southern LIS margin likely stabilized near the St. Lawrence, because the oldest terrestrial organic material from southeastern Quebec dates to 8.7±0.3 kyr BP (2 dates). Farther east, the southern Labrador coast deglaciated before 11.2±0.4 kyr BP (2 marine dates) with the ice margin remaining near the coast until sometime before 8.6±0.7 kyr BP (2 terrestrial dates). Along the northeastern side of the LIS, [10]Be dates indicate ice retreat from the northeastern Labrador coastal moraines at 13.4±1.5 kyr BP (7 dates) and 12.0±2.1 kyr BP (6 dates)[22]. The oldest terrestrial radiocarbon dates from near the coast indicate that ice may have persisted there until 9.9±0.3 kyr BP (6 dates). In contrast, ice over Hudson Bay and the western LIS margin continued to thin and retreat during the early Holocene with the only firm chronologic constraint being the collapse of ice over Hudson Bay 8.5±0.2 kyr BP[21].

Following this collapse, the LIS split into two ice caps: one over Quebec and Labrador, the second over eastern Nunavut and Baffin Island (Fig. 2a). A gap in minimum limiting radiocarbon ages suggests the Quebec/Labrador Ice Cap margins

subsequently stabilized. The southern Quebec margin resumed northward retreat before

7.5±0.2 kyr BP (3 dates) and southern to central Quebec deglaciated before 7.1±0.1 kyr

BP (2 dates). Three dates from eastern Labrador indicate ice margin retreat resumed

before 7.5±0.1 kyr BP, and western to central Labrador deglaciated before 6.6±0.4 kyr

BP (3 dates). Thirteen [10]Be dates and the timing of the marine limit from western

Quebec suggest a similar retreat history, with deglaciation of the James Bay coast by

8.0±0.2 kyr BP followed by margin stabilization[14]. The western margin resumed retreat

~7.4 kyr BP with deglaciation across western to central Quebec 6.8±0.2 kyr BP[14]. To the

northwest, three marine shell dates place the marine incursion in northeastern Nunavut at

7.2±0.1 kyr BP, indicating deglaciation prior to the incursion. Small ice caps likely

persisted over northern Quebec and Labrador until some time before 5.7±0.2 kyr BP (4

dates) and 5.5±0.2 kyr BP (1 date), respectively, and ice over Baffin Island continued to

retreat until ~6 kyr BP[23]. These small ice caps likely constituted <0.5 m of sea level rise[7].

Based on the above chronology, we suggest that two intervals of retreat and

enhanced melting of the LIS occurred in the early Holocene, and place the end of

significant LIS melting at 6.8±0.3 kyr BP (Fig. 1c). The onset of the first enhanced

retreat period presumably began after the Younger Dryas cold event ended ~11.5 kyr BP

and more likely closer to ~9 kyr BP based upon the radiocarbon dates, culminating in the

opening of Hudson Bay ~8.5 kyr BP (Fig. S2). Much of this early melting was likely

focused along the southwestern to western LIS margin and over Hudson Bay, possibly

related to the 0.4-0.6 ‰ decrease in Labrador Sea planktonic δ^{18}O (*Globigerina*

bulloides) (reduced surface water density)[24-26] at ~10-8.4 kyr BP with peak δ^{18}O

depletion ~9 kyr BP (Fig. 1b). After a period of margin stabilization, which may

represent a response to regional reorganization of atmospheric circulation patterns

following the opening of Hudson Bay[14] and cooling from the drainage of Glacial Lake

Agassiz with attendant reduced Atlantic meridional overturning circulation

(AMOC)[12,21,25-27], retreat of the LIS resumed ~7.6 kyr BP and ended ~6.8 kyr BP (Fig

S2). This latter period of melting may also be reflected in the Labrador Sea as a 0.2-0.3

‰ decrease in $\delta^{18}O$ (Fig. 1b).

Laurentide Ice Sheet Contributions To Sea Level Rise

We estimate the LIS Holocene sea level rise contribution by converting LIS area[20]

(km^2), with revised area ages matching our LIS chronology (Fig. S2), to ice volume

(km^3) using the well-established relationship for an ice sheet on a hard bed[28]

(log[volume]=1.23[log[area]-1]). Although this assumes an ice sheet is in equilibrium,

this relationship was developed on ice sheets and ice caps with both negative and positive

mass balances, single and multiple ice domes, a span 4 orders of magnitude in area

(Antarctic Ice Sheet to the Barnes Ice Cap), and climate conditions from temperate

maritime (Iceland) to polar desert (Antarctica). The error in the volume estimate is

~12%, which places the empirically predicted 11 kyr BP ice volume in agreement with

LIS volumes reconstructed by a physically based steady-state ice sheet model[7] and an

isostatic rebound model[15].

From 11 to 6 kyr BP, sea level rose at an average rate of ~1 cm yr^{-1} largely

reflecting melting of the LIS and Antarctic Ice Sheet, with higher rates during the early

Holocene than mid Holocene[15-17] (Fig. 1e). Between 11 and 9 kyr BP, we estimate the

LIS contributed 15±1.8 m of sea level rise at 0.7-0.9 cm yr^{-1} (Fig. 1d & e). During the

subsequent phase of rapid LIS retreat 9-8.5 kyr BP, the LIS contributed 6.6±0.8 m of sea

level rise at ~1.3 cm yr^{-1}. This rate is comparable to geologic evidence for global sea

level rise for this interval derived from coral records[16,17] (Fig 1d). Estuarine records from

Chesapeake Bay[18] also indicate a marsh drowning event ~8.9 kyr BP not explained by isostasy with sea level rising at $\geq$1.2 cm yr^{-1}, similar to our estimated rate of sea level rise from the LIS. After 8.5 kyr BP, the remaining 9.2±1.1 m of LIS sea level rise was added over ~1.7 kyrs. The LIS chronology and Labrador Sea δ^{18}O records suggest a deceleration of retreat ~8.5-7.6 kyr BP with a subsequent increase, corresponding to a LIS contribution to sea level rise of ~0.4 cm yr^{-1} 8.5-7.6 kyr BP, increasing to ~0.7 cm yr^{-1} 7.6-6.8 kyr BP (Fig. 1d). Accelerated LIS retreat 7.6-6.8 kyr BP corresponds with a second increase in the rate of Holocene sea level rise ~7.6 kyr BP[19], when sea level rose ~4.5 m at ~1.0 cm yr^{-1}, suggesting that the LIS was also the main source of sea level rise at this time[14].

Impact Of Early Holocene Climate On The Laurentide Ice Sheet

To quantify the effects of enhanced boreal summer insolation on the LIS and climate, we simulated the 9 kyr BP climate, with a prescribed LIS[7] (Fig. 2a), using the fully coupled atmosphere-ocean general circulation model (AOGCM), NASA Goddard Institute for Space Studies ModelE-R[29]. This model contains a fully coupled surface energy and moisture balance over land ice, but does not include any horizontal ice advection, limiting our analysis to the estimation of the LIS surface mass balance. Additionally, the model tracks water isotopes throughout the hydrologic cycle[29]. To test the skill of the model at simulating 9 kyr BP climate, we compared simulated $\Delta\delta^{18}$O (9 kyr BP – Pre-Industrial[29] (PI)) against a compilation of $\Delta\delta^{18}$O from geologic data (Fig. 3c & f). We compiled Early Holocene (EH, 8-10 kyr BP) and Late Holocene (LH, 3-0 kyr BP) δ^{18}O from ice cores, lake cores, and speleothems, and estimated seawater δ^{18}O (δ^{18}O$_{sw}$) from paired Mg/Ca-based sea surface temperature (SST) and δ^{18}O$_{calcite}$ measurements on the calcite shells of planktonic foraminifera (Supplementary Online

material for a full discussion of methods of data model comparison and model results). Simulated $\Delta\delta^{18}O$ are in agreement with the EH-LH $\Delta\delta^{18}O$ (R^2=0.83) (Fig. 3a). Given the coarse resolution of the AOGCM, this correlation between data and predictions provides confidence in the ability of the model to simulate regional aspects of 9 kyr BP climate, hydrology and LIS surface mass balance.

ModelE-R simulates low $\delta^{18}O_{sw}$ (Fig. 3f), $\delta^{18}O_{calcite}$ and reduced sea surface salinity (not shown) across the northern North Atlantic, Labrador Sea and Arctic Ocean related to the negative LIS mass balance and enhanced run-off, in agreement with North Atlantic paleohydrology data[12-14,26]. The alteration in ocean density suppresses deep winter convection in the Labrador Sea, decreasing total AMOC by ~15% relative to present, also in agreement with interpretations of Labrador Sea deepwater proxies[13]. Reduced AMOC yields relatively cooler temperatures over the Labrador Sea (1-2 °C in the winter, 0.5-1 °C in the summer) extending eastward into the northern North Atlantic (Fig. 3b & d), matching early Holocene paleoclimate reconstructions[10,11]. Further contributing to cooler temperatures is the influence of LIS elevation and albedo, with surface air temperature (SAT) up to 13.5 °C cooler over the ice sheet in the summer, of which 1-2 °C is due to the ice albedo effect (Fig. 3b). The high-pressure system over the LIS maintains an anti-cyclone, reversing wind patterns over Canada (Fig. S3a). The LIS topography forces the mid-latitude jet southward and increases the jet strength (Fig. S3b). Outside of the northern North Atlantic, the Northern Hemisphere summer SST and SAT rise in response to enhanced boreal summer insolation (Fig. 3b & d), amplified by a ~5% reduction in Arctic summer sea ice (Fig. 3e).

The 9 kyr BP simulated annual LIS surface mass balance is -260 cm yr^{-1}, with accumulation zones centered over Quebec, Labrador and eastern Nunavut (Fig. 2b).

Much of the LIS mass reduction is over Hudson Bay where low-elevation ice is lost at rates ranging 11-71 mm day^{-1}, in reasonable accord with our inferences from the LIS chronology. Integrating this LIS mass loss from 9 to 8.5 kyr BP results in ~6 m of sea level rise at ~1.3 cm yr^{-1}, similar to estimates from the LIS chronology (Fig. 1).

Implications For Future Sea Level Rise

The agreement between our interpretations from geologic data and the 9 kyr BP AOGCM that does not include ice dynamics suggests that ice sheets (i.e. the LIS) may have melted rapidly in the past. The inclusion of ice dynamics (e.g., ice streaming) in the 9 kyr BP AOGCM would likely only enhance the melt rate[2]. However, by the early Holocene, much of the LIS was on a hard bed where ice streaming is rare (but not absent), implying that ablation controlled LIS mass balance during this time interval. The AOGCM predicts that a boreal summer shortwave radiative forcing of ~40 W m^{-2} relative to present at the top of the atmosphere[6] can cause considerable summer warming (1-3 °C), promoting a negative mass balance and accelerated melting of a terrestrial ice sheet. Direct comparison to simulations of 2100 C.E. climate (i.e. Special Report on Emissions scenario A1B)[1] is difficult because of a complicated suite of forcings including greenhouse gases, black carbon, ozone, snow albedo, atmospheric H$_2$O, aerosols and land use[30]. However, the cumulative effect is that the increased downward longwave radiation over the Greenland Ice Sheet (GIS) (~10 W m^{-2})[30] is roughly half the surface shortwave radiation changes on the LIS at 9 kyr BP (~20 W m^{-2}), but the summer SAT warming (2-4 °C)[30] is similar in both cases.

Additionally, the different sizes of the early Holocene LIS and the GIS combined with their geographical settings, though they both rest on hard beds predominately above sea level, complicate direct inferences. The GIS is situated in the center of the North

Atlantic with a greater portion of its margin terminating near the ocean, whereas only the eastern and northern LIS margins were near the coast, with the southwestern margin terminating in proglacial lakes. The modern GIS is also ~3 times smaller than the LIS at the start of the Holocene[7,15], but the LIS was similar in size ~8 kyr BP. Currently, ablation, ice streaming and calving control GIS mass loss[2]. However, ice streaming and calving will decrease or cease if the GIS retreats inland[4], making it more analogous to the LIS[7]. Nevertheless, predictions of the rate of sea level rise from the GIS by the end of this century in the A1B scenario[1] are 6 to 40 times smaller than the estimated rate of LIS mass loss in the early Holocene. Given the similar summer SAT responses for these two periods, and the geologic evidence for rapid early Holocene LIS retreat, current projections of GIS melt rates for the coming century may be only minimum estimates even without considering positive feedbacks from ice sheet dynamics.

Methods

We simulate climate using the fully coupled AOGCM NASA Goddard Institute for Space Studies ModelE-R, which includes water isotopes[29], permitting direct comparison to marine and terrestrial $\delta^{18}O$ records. Because a true transient simulation from the Last Glacial Maximum -- even assuming that the glacial maximum was in equilibrium -- to 9 kyr BP is beyond our current computational power, we performed a time-slice simulation of 9 kyr BP climate. Boundary conditions appropriate to 9 kyr BP are prescribed (greenhouse gases, insolation, LIS topography, 40 m of sea level lowering and its effects on ocean salinity and $\delta^{18}O$, and the addition of Glacial Lake Agassiz), with details provided in the Supplementary Online Materials. ModelE-R has a simple ice sheet scheme that includes ice sheet surface albedo and energy, freshwater, and water isotopes, with two snow/ice layers that transfer heat and mass. Net melt is transported

through a 9 kyr BP-appropriate river routing scheme based on LIS topography and North American isostasy[7]. Ideally, a higher resolution model with ice dynamics would be employed, but these usually use simplified predictions of summer melt and are asynchronously coupled to GCMs[3,4], not allowing the ice sheet hydrology to directly communicate with the atmosphere and ocean systems. Within the model, there is an imposed global water balance, which modulates the ice calving term to prevent long-term salinity drift in the ocean, with the Southern and Northern Hemispheres partitioned separately. Thus in the model experiment the negative LIS surface mass balance is compensated by a reduction in Northern Hemisphere iceberg calving from the GIS, and therefore, likely underestimates the total ice sheet impact on ocean outflow. ModelE-R was run for 600 model years with results from the last 100 years averaged and compared to a corresponding 100-year average of the Pre-Industrial[29]. Differences between 9 kyr BP and Pre-Industrial[29] were calculated using a student-t test at 99% confidence.

1. IPCC in *Climate Change 2007: The Physical Basis* 4th Assessment Report, IPCC (eds Solomon, S.D. & Manning, Qin M.) 18 p. (Cambridge University Press, 2007).

2. Alley, R.B., Clark, P.U., Huybrechts, P. & Joughin, I. Ice-Sheet and Sea-Level Changes. *Science* **310**, 456-460 (2005).

3. Wild, M., Pierluigi, C., Scherrer, S.C., & Ohmura, A., 2003. Effects of polar ice sheets on global sea level in high-resolution greenhouse scenarios. *J. Geophys. Res.* **108**, doi: 10.1029/2002JD002451.

4. Ridley, J.K., Huybrechts, P., Gregory, J.M., & Lowe, J.A., 2005, Elimination of the Greenland Ice Sheet in a High CO_2 Climate. *J. Climate* **18**, 3409-3427.

5. Gregory, J.M., Huybrechts, P., & Raper, S.C.B., 2004, Threatened loss of the Greenland ice-sheet. *Nature* **428**, 616.

6. Berger, L. & Loutre, M.F. Insolation values for the climate of the last 10 million years. *Quat. Sci. Rev*. **17**, 211-219 (1991).

7. Licciardi, J.M., Clark, P.U., Jenson, J.W. & MacAyeal, D.R. Deglaciation of a soft-bedded Laurentide Ice Sheet. *Quat. Sci. Rev*. **17**, 427-488 (1998).

8. Mitchell, J.F.B., Grahame, N.S. & Needham, K.J. Climate simulations for 9000 years before present: Seasonal variations and effect of the Laurentide Ice Sheet. *J. Geophys. Res. Atm.* **93**, 8283-8303 (1988).

9. Pollard, D., Bergengren, J.C., Stillwell-Soller, L.M., Felzer, B. & Thompson, S.L. Climate simulations for 10,000 and 6,000 years BP. *Paleoclimates* **2**, 183-218 (1998).

10. Kaufman D.S. et al. Holocene thermal maximum in the western Arctic (0-180ºW). *Quat. Sci. Rev*. **23**, 529-560 (2004).

11. Kaplan, M.R. & Wolfe, A.P. Spatial and temporal variability of Holocene temperature in the North Atlantic. *Quat. Res*. **65**, 223-231 (2006).

12. Came, R.E., Oppo, D.W. & McManus, J.F. Amplitude and timing of temperature and salinity variability in the subpolar North Atlantic over the past 10 k.y. *Geology* **35**, 315-318 (2007).

13. Hillaire-Marcel, C., deVernal, A., Bilodeau, G. & Weaver, A.J. Absence of deep-water formation in the Labrador Sea during the last interglacial period. *Nature* **410**, 1073-1077 (2001).

14. Carlson, A.E., Clark, P.U., Raisbeck, G.M. & Brook, E.J. Rapid Holocene Deglaciation of the Labrador Sector of the Laurentide Ice Sheet. *J. Climate* **20**,

5126-5133 (2007).

15. Peltier, W.R. Global Glacial Isostasy and the Surface of the Ice-Age Earth: The ICE-5G (VM2) Model and GRACE. *Annu. Rev. Earth Planet. Sci*. **32**, 111-149 (2004).

16. Fairbanks, R.G. A 17,000 year glacio-eustatic sea level record: Influence of glacial melting rates on the Younger Dryas event and deep ocean circulation. *Nature* **342**, 637-642 (1989).

17. Bard, E.B. et al. Deglacial sea-level record from Tahiti corals and the timing of global meltwater discharge. *Nature* **382**, 241-244 (1996).

18. Cronin, T.M. et al. Rapid sea level rise and ice sheet response to 8,200-year climate event. *Geophys. Res. Lett*. **34** doi:10.1029/2007GL031318 (2007).

19. Yu, S.-Y., Berglund, B.E., Sandgren, P. & Lambeck, K. Evidence for a rapid sea-level rise 7600 yr ago. *Geology* **35**, 891-894 (2007).

20. Dyke, A.S. in Quaternary Glaciations-Extent and Chronology Part II Vol. 2b (eds Ehlers, J. & Gibbard, P.L.) 373-424 (Elsevier, Amsterdam, 2004).

21. Barber, D.C. et al. Forcing of the cold event of 8,200 years ago by catastrophic drainage of Laurentide lakes. *Nature* **400**, 344-348 (1999).

22. Clark, P.U., Brook, E.J., Raisbeck, G.M., Yiou, F. & Clark, J. Cosmogenic [10]Be ages of the Saglek Moraines, Torngat Mountains, Labrador. *Geology* **31**, 617-620 (2003).

23. Miller, G.H., Wolfe, A.P., Briner, J.P., Sauer, P.E. & Nesje, A. Holocene glaciation and climate evolution of Baffin Island, Arctic Canada. *Quat. Sci. Rev*. **24**, 1703-1721 (2005).

24. Hillaire-Marcel, C. & Bilodeau, G. Instabilities in the Labrador Sea water mass

structure during the last climatic cycle. *Can. J. Earth Sci*. **37**, 795-809 (2000).

25. Hillaire-Marcel, C., deVernal, A. & Piper, D.J.W. Lake Agassiz final drainage event in the northwest North Atlantic. *Geophys. Res. Lett*. **34** doi:10.1029/2007GL030396 (2007).

26. Keigin, L.D., Sachs, J.P., Rosenthal, Y. & Boyle, E.A. The 8200 year B.P. event in the slope water system, western subpolar North Atlantic. *Paleoceanography* **20**, doi: 10.1029/2004PA001074 (2005).

27. LeGrande, A.N. et al. Consistent simulations of multiple proxy responses to an abrupt climate change event. *Proc. Natl. Acad. Sci*. **103**, 837-842 (2006).

28. Paterson, W.S.B. The Physics of Glaciers (Butterworth-Heinemann, Oxford, UK, 1994).

29. Schmidt, G.A., LeGrande, A.N. & Hoffmann, G. Water isotope expressions of intrinsic and forced variability in a coupled ocean-atmosphere model. *J. Geophys. Res. Atm.* **112**, doi:10.1029/2006JD007781 (2007).

30. Hansen, J. et al. Dangerous human-made interferences with climate: a GISS modelE study. *Atmos. Chem. Phys.* **7**, 2287-2312 (2007).
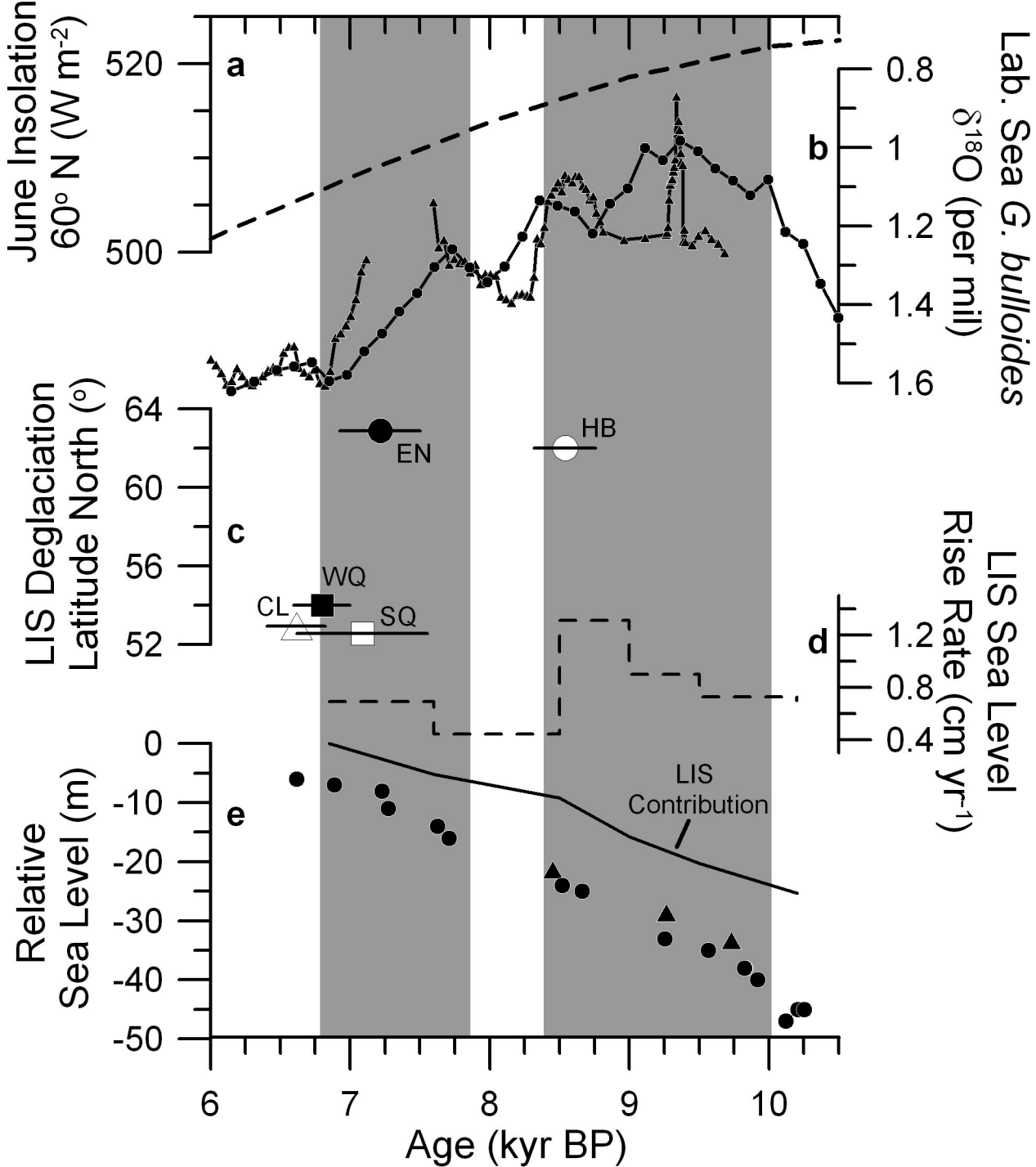
Author Contributions. A.E.C. compiled terrestrial and marine records of LIS retreat. A.N.L. & G.A.S. developed the AOGCM model. A.N.L. initiated and analyzed the 9 kyr BP simulations. A.N.L., G.A.S., A.E.C. & J.M.L. designed model boundary conditions. A.E.C., R.E.C., E.A.O. & D.W.O. compiled oxygen isotope data. A.N.L., A.E.C. & F.S.A. interpreted LIS mass balance. All authors collaborated on the text.

Author Information. Correspondence and requests for materials should be addressed to A.E.C.

Figure 1. Early Holocene Terrestrial and Marine Records. (**a**) 60º N June insolation[6]. (**b**) *G. bulloides* $\delta^{18}O_c$ records with ice volume removed[16] from southwestern Labrador Sea (circles: MD95-2024, 50.21º N, 45.69º W, water depth 3539 m[24], triangles: MD99-2237, 50.20º N, 45.68º W, water depth 3530 m[25]). (**c**) LIS deglaciation relative to Latitude North: acronyms are HB=Hudson Bay[21], WQ=western Quebec[14], SQ=southern Quebec[20], CL=central Labrador[20], EN=eastern Nunavut[20]. (**d**) Rate of sea level rise from the LIS. (**e**) Relative sea level data (triangles from Barbados[16], circles from Tahiti[17]) and changes in LIS volume (black line). Gray bars denote periods of increased LIS melting.
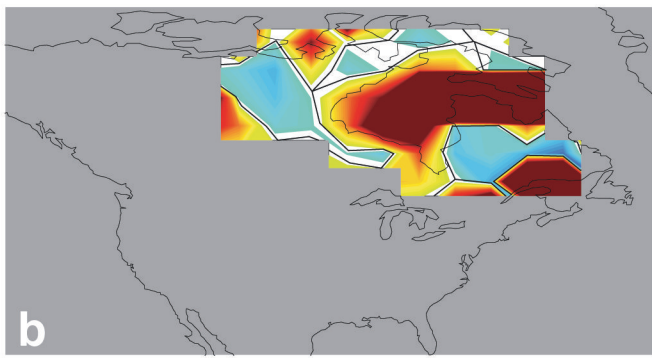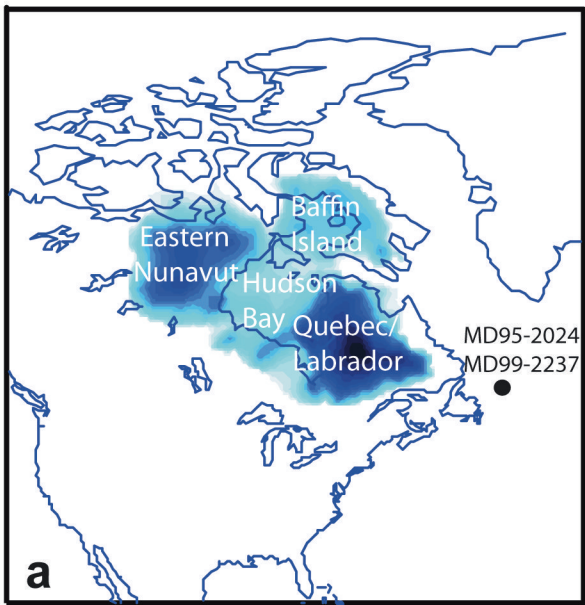
Figure 2. Laurentide Ice Sheet Topography and Mass Balance. (**a**) LIS topography[7] (m) used as AOGCM input with regions labeled and the locations of MD95-2024 & MD99-2237. (**b**) ModelE-R simulated annual mass balance predicted (mm day^{-1}) with the black lines denoting the equilibrium line.

Figure 3. ModelE-R Output Delta Maps between 9 kyr B.P. and PI. (**a**) Comparison

between paleo-$\Delta\delta^{18}$O precipitation and seawater changes between the Early Holocene

(EH) and Late Holocene (LH) (see 3c and 3e for locations) and ModelE-R 9 kyr BP-PI

predicted changes. Dashed line is 1:1 relationship. See Table S2 for data. (**b**) ModelE-R

ΔSAT summer. (**c**) ModelE-R $\Delta\delta^{18}O_{pr}$ annual (ice volume removed). (**d**) ModelE-R

ΔSST summer. (**e**) ModelE-R Δsummer sea ice extent. (**f**) ModelE-R $\Delta\delta^{18}O_{sw}$ annual

(ice volume removed).

Laurentide Ice Sheet 9 kyr BP

Meters

Baffin
Island

Eastern
Nunavut

Hudson
Bay

Quebec/
Labrador

MD95-2024
MD99-2237

a

b

LIS 9 kyr BP Mass Balance (mm/day)

-70.5 -5 -4 -3 -2 -1 -.4 .4 1 2 3 4 5 6

a — Scatter plot: $\Delta\delta^{18}O$ (EH-LH) versus ModelE-R $\Delta\delta^{18}O$ (9 ka - PI)

Legend:
- Seawater (black square)
- Ice Core (blue circle)
- Speleothem (red triangle)
- Lake (green diamond)

b — Δ 9K JJA SAT (C)

Color scale: −12.9 −3.4 −2.5 −1.6 −.9 −.3 .3 .8 1.2 1.8 2.4 3 3.5 4.1 13

c — Δ 9K ANN $\delta^{18}O_{pr}$ (permil)

Legend:
- Ice Core
- Speleothem
- Lake Core

Color scale: −10.7 −2.3 −1.7 −1.1 −.6 −.2 .2 .5 .8 1.3 1.7 2.2 2.7 5.4

d — Δ 9K JJA SST (C)

Color scale: −5.7 −3.6 −2.7 −1.8 −1 −.4 .3 .8 1.2 1.8 2.4 3 3.5 4.1 14.5

e — Δ 9K JJA ICE (%)

Color scale: −98.5 −3.4 −2.5 −1.6 −.9 −.3 .3 .8 1.2 1.8 2.4 3 3.5 4.1 76.9

f — Δ 9K ANN 0m $\delta^{18}O_{sw}$ (permil)

Legend:
- Ocean Core

Color scale: −8 −2.5 −2 −1.5 −1 −.6 −.2 .2 .5 .8 1.3 1.7 2.2 2.7 3